OPTIC FIBER SENSOR FOR STRAIN MEASUREMENTS IN HIGH TEMPERATURE SENSING APPLICATIONS

Julia White
Department of Electrical and Computer Engineering
Missouri University of Science and Technology
Rolla, MO, 65401
jwk8f@mst.edu

Faculty Advisors:
Jie Huang, Kurt Kosbar

ABSTRACT

Optic fiber sensors are employed in a variety of applications for the remote measurement of various parameters such as strain, pressure, or temperature. These sensors offer an array of benefits as well including light weight, compactness, and high resolution. In particular, Fabry-Perot interferometers (FPIs) maintain these benefits and can also be made to withstand extremely high temperatures. This advantage of the FPI allows it to be used in harsh environments where many other tools for parameter measurement could not survive. An FPI strain sensor is constructed and tested which has the capabilities to be used at high temperatures of over 1000°C for applications in gas turbine engine testing. This paper discusses the need for high temperature strain sensors in engine testing and this sensor's capabilities in this application.

INTRODUCTION

Strain measurements are required in various applications with harsh, high temperature, environments. While high temperature strain gauges exist on the market to meet these needs, most have limits ranging from 400 to 800 °C which can't withstand temperatures encountered in certain cases of engine testing. However, the Fabry-Perot interferometer (FPI) can be used as a strain sensor in these environments due to its ability to withstand high temperatures of over 1000 °C.

FPIs are well suited for applications in engine testing due to the benefits of optic fiber sensors (light weight, compactness, and high resolution [1]), and also for their high temperature thresholds [2]. The purpose of this paper is to show the capabilities of FPIs in terms of strain measurement for the high temperature conditions that occur in engine testing. This paper will demonstrate these capabilities through an explanation of the theory behind using FPIs for gas turbine engine testing and an explanation of the construction and testing of a FPI.

A SUMMARY OF THE FABRY-PEROT INTERFEROMETER

A FPI consists of two parallel reflective surfaces that can be used to measure various physical parameters such as strain, pressure, or temperature [3,4]. These measurements are based off of an interference pattern. The interference pattern is created when light waves reflected off of the two surfaces interfere with each other due to their different delays. This pattern can be analyzed to remotely determine the values of the aforementioned physical parameters by observing changes in the resulting waveform's phase, light intensity, or wavelength. In particular, changes in strain on an FPI result in a phase shift caused by distortion of the light being reflected off of the two parallel surfaces. Strain on the FPI physically lengthens the space between the reflective surfaces which causes this distortion. This is modeled by the formula for strain, ε, given in Equation (1).

$$\varepsilon = \Delta_L/L = \Delta_\lambda/\lambda \quad (1)$$

Where l is distance, Δ_L is the change in distance, λ is wavelength at a certain point on the wave when there is no strain, and Δ_λ is the change in wavelength (phase shift) of this point when there is ε strain. Using (1), we can determine a value of strain with only the initial waveform where strain is zero and a secondary waveform where strain is ε. These waveforms are illustrated in Figure 1.

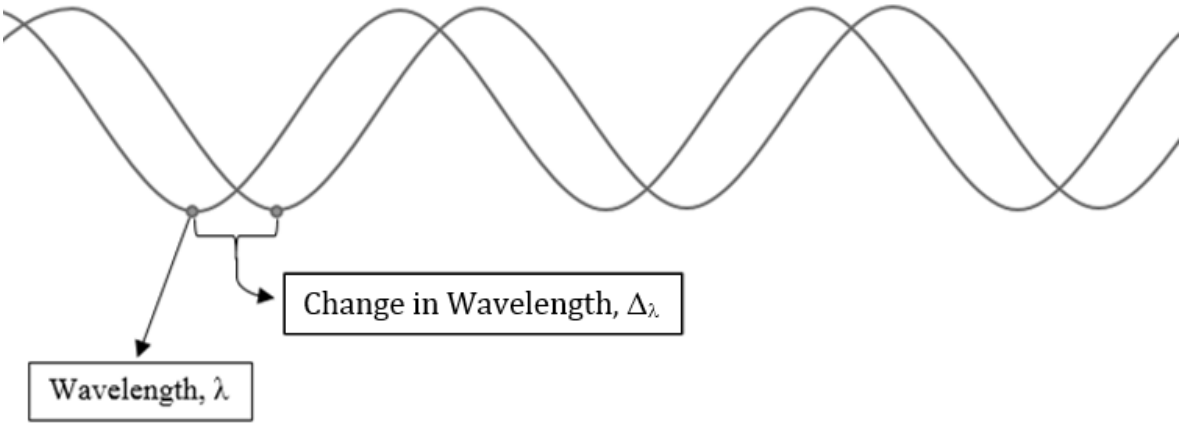

Figure 1 Waveforms Illustration

In addition to strain the FPI can also be used to measure other parameters such as temperature (which has interrelated effects on the interference pattern). Because of this, FPIs have been designed to measure and withstand extremely high temperatures of over 1000 °C using various methods of construction [2]. In the case of a FPI made with glass tubing, since glass fibers have extremely high melting points, a particular fiber could withstand up to 1200 °C before softening.

THEORY BEHIND IMPLEMENTATION IN GAS TURBINE ENGINE TESTING

Gas turbine engines reach temperatures of up to 2000 °C at their core due to the high temperatures produced by burning fuel. However, since the metals used in most jet engines begin

to melt at 1300 °C, cooling mechanisms are implemented in order to keep temperatures below that threshold [5,6]. These temperatures are manageable for many variations of the FPI model.

FPIs can be constructed to withstand temperatures above 1000 °C, which makes them a good solution for gathering strain measurements in high temperature gas turbine engines where most strain gauges are not suitable. Temperature does have certain effects on the interference pattern of an FPI though. FPIs designed for measuring temperature typically have a cavity material with a temperature-dependent refractive index. This needs to be accounted for when taking strain measurements because temperature will alter the phase shift produced by a certain strain (i.e. the same strain value will show different wavelengths for a given peak at different temperatures) [7,8]. In order to accurately use the phase shift of the interference signal to measure strain, the FPI must be calibrated before measuring strain at different temperatures by using a temperature sensor in conjunction near the FPI. The measurements can then be used to account for the temperature strain cross-sensitivity of the FPI (which is a value in units of microstrain/°C and will vary for different constructions) and calculate strain.

FPI CONSTRUCTION

The FPI implemented in this report is a simple design which consists of single mode fiber and glass tubing. The FPI was prepared by first fusing a single mode fiber with a section of glass tubing. Then, the glass segment was cleaved under a microscope to the length of approximately 100 microns. After that, the cleaved end of the glass tubing was fused to another single mode fiber as shown in Figure 2.

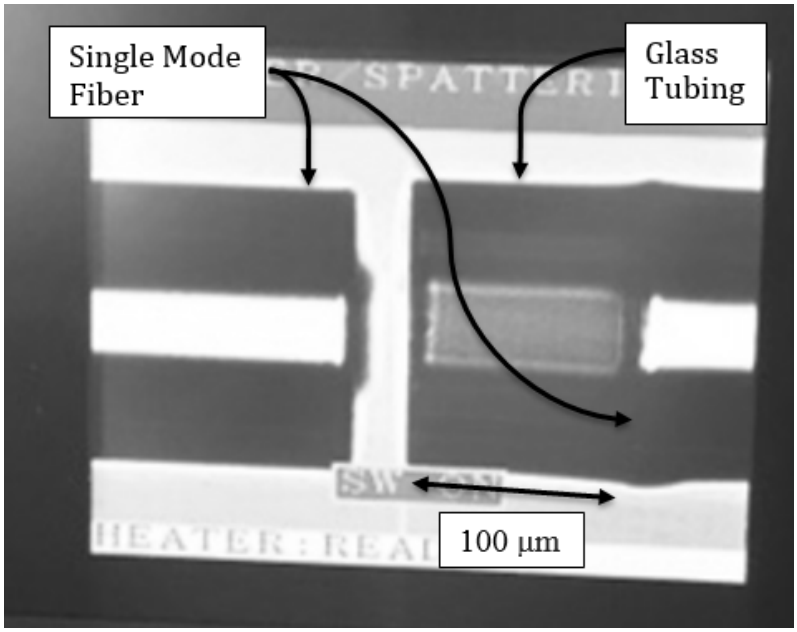

Figure 2 Fusing Single Mode Fiber with Glass Tubing

The surfaces where the fiber and glass tubing were fused together act as reflective surfaces. These surfaces reflect light with different delays which results in the interference pattern that is used to measure strain. Figure 3 depicts this construction.

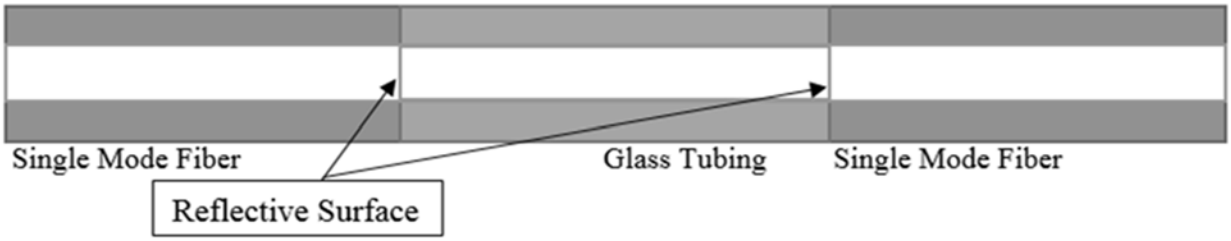

Figure 3 Fabry-Perot Interferometer

STRAIN TESTING

Strain testing of the FPI was performed with the use of an optical spectrum analyzer and a broadband ASE (Amplified Spontaneous Emission) light source. The single mode fiber on one end of the FPI was connected to the light source and the other end was connected with the spectrum analyzer. The resulting waveform displayed on the spectrum analyzer was irregular due to the varying amplitudes of the ASE light source. In order to normalize the waveform used for analysis, the FPI's output waveform was subtracted by the light source's waveform in the spectrum analyzer. This produced a stable sine wave which was recorded and used for calculations. The spectrum analyzer and light source connections are shown in Figure 4.

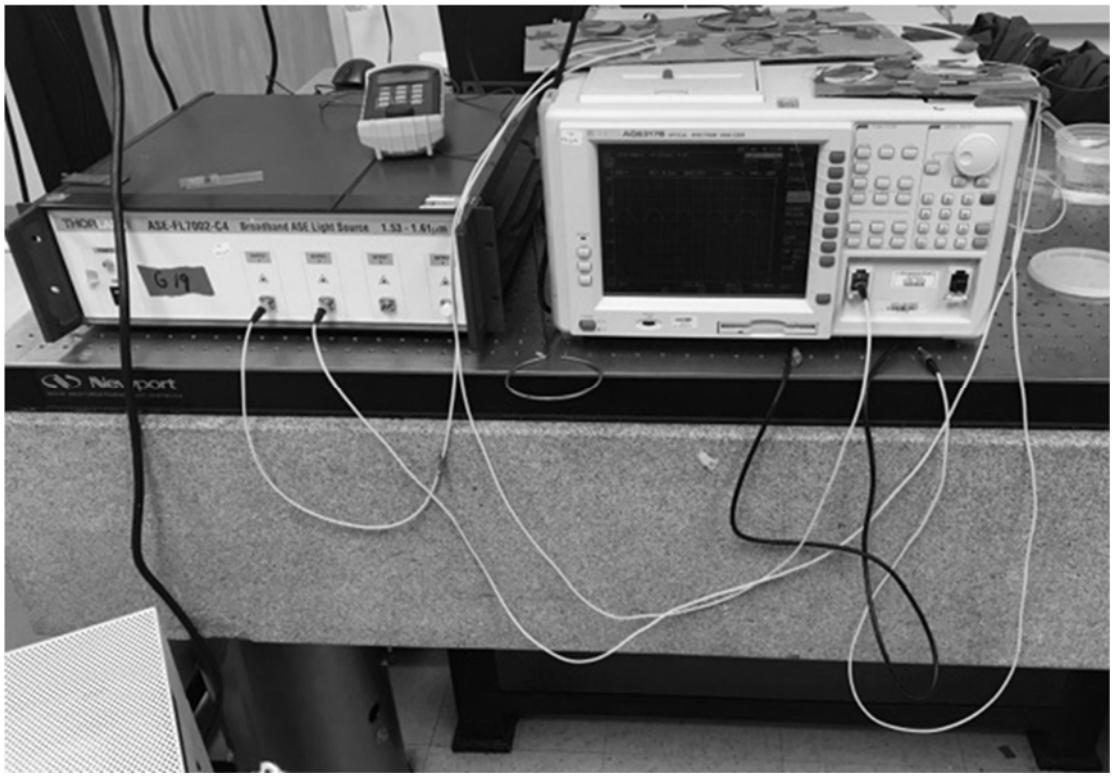

Figure 4 Spectrum Analyzer Connections

With the spectrum analyzer set up, the FPI was then glued with an epoxy resin onto two moveable plates as shown in Figure 5. After drying the epoxy, the waveforms were recorded as the plates were shifted apart in increments of approximately 0.025mm, slowly stretching the FPI. This stretching produced strain which could be measured by both the length of the FPI and wavelength measurements gathered on the spectrum analyzer.

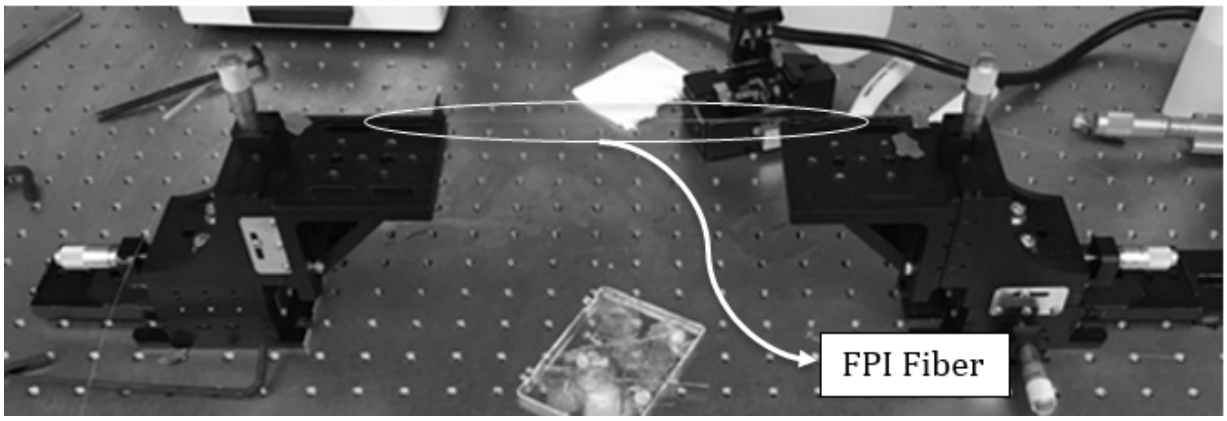

Figure 5 FPI Fixed to Moveable Plates

RESULTS AND ANALYSIS

The output waveforms gathered from the spectrum analyzer were recorded as the strain was increased. Four of the eleven waveforms gathered over eleven trials with varying strains are shown in Figure 6 to demonstrate the phase shift observed as strain increases. The trials depicted below (trials 0, 3, 6, and 10) are labeled with the FPI's change in length (Δ_L).

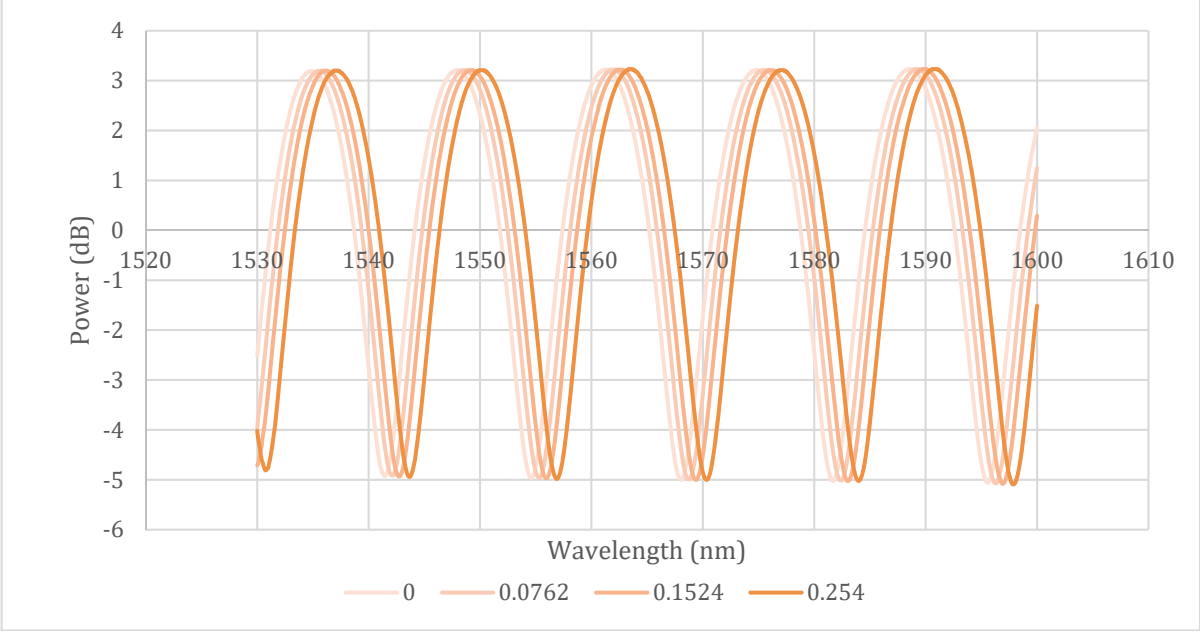

Figure 6 FPI Strain Testing Output Waveforms

A simple zero crossing technique was used to determine the phase shift of the waveform as strain increased. This method, rather than some more complicated signal processing techniques for calculating phase shift, was sufficient since the data presented in this report has a high signal to noise ratio. The third zero-crossing of the trial 0 (no strain) waveform was used as a reference point and its change in wavelength (Δ_λ) was tracked through the following ten trials.

Table 1 FPI Strain Testing Derived Values

Trial	Δ_L (mm)	Δ_L/L	Δ_λ (nm)	Δ_λ/λ	Percent Error (%)
0	0	0	0	0	0
1	0.0000254	0.000141	0.21	0.000136	3.623442
2	0.0000508	0.000282	0.455	0.000295	-4.40794
3	0.0000762	0.000423	0.665	0.000431	-1.73081
4	0.0001016	0.000564	0.91	0.000589	-4.40794
5	0.000127	0.000706	1.05	0.00068	3.623442
6	0.0001524	0.000847	1.295	0.000839	0.946316
7	0.0001778	0.000988	1.505	0.000975	1.328762
8	0.0002032	0.001129	1.75	0.001133	-0.39225
9	0.0002286	0.00127	1.995	0.001292	-1.73081
10	0.000254	0.001411	2.24	0.001451	-2.80166
					λ = 1544.14 nm
					L = 180 mm

Table 1 gives values for the change in wavelength of the third lower peak (Δ_λ) and length the FPI was stretched (Δ_L) in all 11 trials as well as the initial value for wavelength (λ) and length (L) before any stretching. Values for Δ_L/L and Δ_λ/λ are also given and, by Equation (1), these values both represent strain. These two columns (Δ_L/L and Δ_λ/λ) when compared give the error values listed in the sixth column. With Δ_L/L taken as the theoretical strain value and Δ_λ/λ taken as the experimental strain value, percent error was calculated by Equation (2).

$$\%_E = ((A - E)/A)*100\% \quad (2)$$

Where $\%_E$ is percent error, A is the actual value for strain determined from the FPI length, and E is the experimental value for strain determined by the wavelength. The errors calculated (which range from -4.40794% to 3.623442%) are attributed to random error because the average value for percent error of all 11 trials is within (-)1% of zero at -0.54086% and therefore the error was not consistently in a single direction (which would indicate systematic error). The discrepancies between the two strain calculations are a product of precision limitations that can be attributed to imprecision of the measurements gathered by the spectrum analyzer. This could be minimized with better, more precise, equipment. However, even with random error the accuracy of the strain measurements given by $\Delta\lambda/\lambda$ are consistently within 5% of the actual strain values which shows that the phase shift of these waveforms could be used to relatively accurately (within 95% of the true value) predict strain at constant temperature.

CONCLUSIONS

The Fabry-Perot Interferometer is an alternative solution to taking high temperature strain measurements required in gas turbine engine testing without the use of a strain gage (most of which can't operate at high enough temperatures to accommodate the harsh environments encountered in certain cases of engine testing). The FPI's ability to withstand extreme temperatures and accurately, remotely, measure strain through changes in the interference pattern make it useful in these applications. This paper discussed the theory behind the implementation of FPIs in the high temperature environments which occur in gas turbine engine testing. The strain sensing capabilities of the FPI were also demonstrated as a FPI was constructed and tested for various values of strain. Future work could be performed to demonstrate potential variance in strain measurement limits at different temperatures.

ACKNOWLEDGEMENTS

The laboratory work discussed in this paper was performed with the assistance Yiyang Zhuang, graduate student at Missouri University of Science and Technology in the Electrical and Computer Engineering Department.

REFERENCES

[1] K. Grattan and T. Sun, "Fiber optic sensor technology: an overview," Sensors and Actuators A Physical, vol. 82, iss. 1-3, May, 2000, pp. 40–61.
[2] I. Rajibul, "Chronology of Fabry-Perot Interferometer Fiber-Optic Sensors and Their Applications: A Review," Multidisciplinary Digital Publishing Institute, 14, April, 2014, pp. 7451-7488.
[3] S. Tseng and C. Chen, "Optical fiber Fabry-Perot sensors," Applied Optics, vol. 27, iss. 3, Feb, 1988, pp. 547-551. 10.1364/AO.27.000547

[4] Q. Yu and X. Zhou, "Pressure sensor based on the fiber-optic extrinsic Fabry-Perot interferometer," Photonic Sensors, vol. 1, 2011, pp. 72-83.
[5] "The Jet Engine: A Historical Introduction," Stanford, 16, March, 2004.
[6] T. Jenkins, S. Allison, and J. Eldridge, "Measuring gas turbine engine component temperatures using thermographic phosphorus," SPIE, 20, March, 2013. 10.1117/2.1201303.004769
[7] G. Beheim, "Fiber-Optic Temperature Sensor Using a Thin-Film Fabry-Perot Interferometer," Case Western Reserve University, May, 1997.
[8] L. Yujie, H. Ming, and T. Jiajun, " Fiber-Optic Temperature Sensor Using a Fabry-Perot Cavity Filled With Gas of Variable Pressure," IEEE Photonics Technology Letters, vol. 26, iss. 8, 15, April, 2014, pp. 757-760.